Research Article | Vol. 29, No. 3 / 1 February 2021 / Optics Express 4210
Optics EXPRESS

Saturation control of an optical parametric chirped-pulse amplifier

PETER FISCHER,[1] ALEXANDER MUSCHET,[1] TINO LANG,[2] ROUSHDEY SALH,[1] AND LASZLO VEISZ[1,*]

[1]Department of Physics, Umeå University, SE-90187 Umeå, Sweden
[2]Deutsches Elektronen-Synchrotron DESY, Notkestraße 85, 22607 Hamburg, Germany
*laszlo.veisz@umu.se

Abstract: Optical parametric chirped-pulse amplification (OPCPA) is a light amplification technique that provides the combination of broad spectral gain bandwidth and large energy, directly supporting few-cycle pulses with multi-terawatt (TW) peak powers. Saturation in an OPCPA increases the stability and conversion efficiency of the system. However, distinct spectral components experience different gain and do not saturate under the same conditions, which reduces performance. Here, we describe a simple and robust approach to control the saturation for all spectral components. The demonstrated optimal saturation increases the overall gain, conversion efficiency and spectral bandwidth. We experimentally obtain an improvement of the pulse energy by more than 18%. This technique is easily implemented in any existing OPCPA system with a pulse shaper to maximize its output.

1. Introduction

In the recent years optical parametric chirped-pulse amplification [1–3] (OPCPA) has become a new standard in laser technology [4–9] extending Titanium-Sapphire (Ti:Sa) laser systems [10,11] in many applications [12–16]. This is due to advantageous properties of OPCPA [17–19] like broad amplification bandwidth, high single-pass gain, high temporal contrast, low thermal load and extended spectral region to the mid-infrared [20–23]. It enables scalable systems with stable carrier-envelope phase (CEP) [5] or even few-cycle pulses at relativistic intensities [24]. The basic structure of an OPCPA system involves a source delivering weak and broadband seed pulses, which are temporally elongated in a stretcher, amplified in optical parametric amplifiers (OPAs) and these signal pulses are shortened in a tailored compressor near to their Fourier limited pulse duration. Saturation in the nonlinear optical crystals of the OPA corresponds to the situation when the pump starts to be depleted and at strongest saturation signal and idler have maximal energy. It has many important advantages, among others provides good pump to signal efficiency, reduces the shot-to-shot energy fluctuations and provides slightly broader signal spectrum. As the broadband pulse is stretched in the OPAs the different wavelength components arrive at different times and saturate independently. The optical-to-optical efficiency is an important measure for such few-cycle systems, which is for OPCPA comparable to short-pulse (20-30 fs) Ti:Sa lasers [10,25]. Experimental few-cycle systems confirm this by reaching up to 26% [9] or even 31% [26] efficiency. To further improve efficiency different techniques have been proposed, which concentrate on the pump laser and nonlinear crystal. The ideas are either to absorb [27], block the idler and reuse the pump [28,29] or tailor the pump spatial and/or temporal shape [30–36]. It was also proposed to shape the pump or seed temporal profile or try to tailor phase matching to reach optimal efficiency for a broadband OPCPA [37]. These (spatial and/or temporal) profiles of the pump and/or seed pulses that maximize efficiency are called ‘conformal profiles’ [37,38]. This theory delivers results sometimes with large improvements compensating for pump temporal shape and phase matching, but the shaping is not feasible in practice.

#415564 https://doi.org/10.1364/OE.415564
Journal © 2021 Received 20 Nov 2020; revised 17 Jan 2021; accepted 18 Jan 2021; published 26 Jan 2021

Optics EXPRESS

Here, we demonstrate experimental optimization of gain saturation by controlling the spectral shape of the seed pulse. In our approach, a simple algorithm scans the spectral transmission in a spectral amplitude and phase shaper, detects the saturation of the different spectral components in a multi-stage OPCPA, and then applies the corresponding optimal spectral transmission function. Possible daily changes of the seed spectrum or slightly different alignment of the OPAs are naturally compensated by matching this transmission function. To obtain the conformal seed temporal profile this experimental way is flexible, results in flat broadband spectra and maximal pump depletion plus it can even be combined with other measures for efficiency improvement.

2. Theory

The small-signal gain G and signal intensity I_s in OPA in the unsaturated regime are calculated by Eqs. (1) and (2):

$$I_s(z) = G(z)I_s(0) = \frac{\Gamma^2}{4g^2} I_s(0) e^{2gz}, \tag{1}$$

$$g = \sqrt{\Gamma - \left(\frac{\Delta k}{2}\right)^2}, \quad \Gamma = \frac{2\omega_s \omega_i {d_{eff}}^2 I_p(0)}{n_s n_i n_p \varepsilon_0 {c_0}^3}, \tag{2}$$

where z is the longitudinal coordinate along propagation direction, $I_s(0)$ is the seed (input signal) intensity, $I_p(0) = I_p(z)$ is the undepleted pump intensity, Γ is the small signal gain coefficient with perfect phase matching, g is the small signal gain coefficient and c_0 is the speed of light. Furthermore, the small-signal gain is in turn dependent on the properties of the nonlinear crystal via d_{eff} the effective nonlinear coefficient and n_s, n_i, n_p the index of refraction of corresponding polarization of signal, idler and pump, ω_s, ω_i the frequencies of signal and idler waves, as well as on the phase mismatch between these three waves in general in a noncollinear geometry $\Delta k = |\boldsymbol{k}_p - \boldsymbol{k}_s - \boldsymbol{k}_i|$. For quasi-monochromatic cases optimal conditions with perfect phase matching can be found. However, a wavelength-dependent phase mismatch has to be accepted, to achieve a broad spectral amplification window. Taking the temporal shape of pump and signal pulses into account, the gain and therefore the output signal intensity is wavelength and pump-intensity dependent.

As most of the amplification is in the linear regime, the former conclusion is valid also if saturation takes place. However, in the optimal case, in contrary to the formerly described typical case, during optimal saturation the depletion of the pump should be maximal at all time instants. As the signal is chirped in OPCPA the different wavelengths arrive at different times to the amplifier. Therefore, optimal saturation at all time instants leads to nearly constant output signal intensity over the amplified spectrum at the exit of the nonlinear crystal. This way the broadest amplified spectrum is achieved, that is supported by the used phase matching geometry and the highest signal energy is reached at the same time by evenly extracting the maximal energy from the pump pulse at all wavelength. Correspondingly, the crystal thicknesses to reach optimal saturation for a common setup depend on the wavelength. An alternative control parameter to realize optimal amplification and saturation is the wavelength-dependent seed intensity, i.e. tuning the amplitude of various spectral components.

3. Simulations

A more complete description of amplification including essential effects in OPCPA such as phase mismatch, saturation, pump depletion and back-conversion can only be modelled by numerically solving the coupled nonlinear wave equations. Two methods are commonly employed for this purpose: Fourier space methods are more accurate, in contrast split-step solvers are a faster and more general approach with the possibility for higher order nonlinear effects [39]. For

Optics EXPRESS

our simulations we used an 2 + 1-dimensional split-step algorithm for generalized ordinary and extraordinary pulses [40].

In a first step, simple monochromatic 1D simulations, based on equations in [1], illustrate the effect of wavelength-dependent small-signal gain as shown in Fig. 1. The parameters for the simulation (see caption Fig. 1) are chosen to be identical to the experimental setup described later. Noncollinear phase matching geometry is applied, which is characterized by the noncollinear angle α between pump and seed wave vectors in the beta barium borate crystal (BBO), the phase matching angle θ between pump wave vector and crystal axis, the azimuthal angle ϕ , and an angularly dispersed idler. For constant seed (dashed for wavelength indicated by orange and red and solid green), the saturation for different wavelengths takes place at different crystal depths. The main reason is the direct frequency dependence of the small signal gain coefficient with perfect phase matching in Eq. (2) ($\Gamma \propto \omega_s \omega_i$), which gives higher gain towards degeneracy at 1064 nm. However, using tailored seed intensity (×1.5 reduction at 800 nm and ×2.2 at 900 nm) saturation is shifted deeper into the crystal towards the wavelength components with lowest gain. In case of a broadband pulse, especially with a realistic spectrum with large intensity changes, this would result in an improved efficiency, energy and even intensity for the compressed pulse.

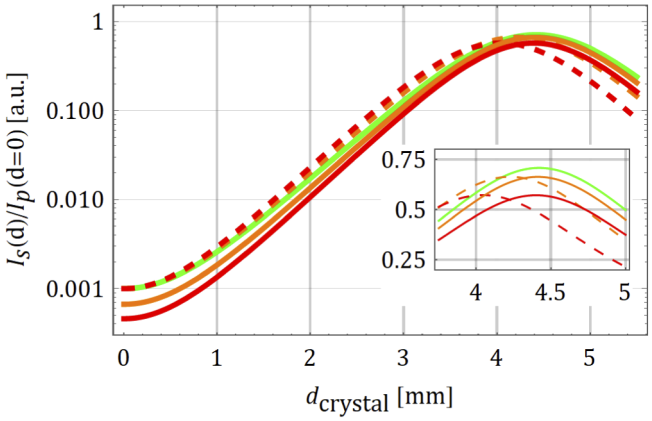

Fig. 1. Simulated signal intensity in BBO ($I_s(0) = 6\text{MW/cm}^2, I_p(0) = 6\text{GW/cm}^2, \lambda_p = 532$ nm, $\theta = 23.7°, \phi = 90°, \alpha = 2.3°$) along the crystal for different signal wavelengths (green – 750 nm, orange – 800 nm, red – 900 nm) and seed (input signal) intensities. For constant intensity (dashed orange, dashed red and solid green), saturation occurs at different thicknesses. Matched input seed intensity (solid) synchronizes saturation at the end of the optimal crystal thickness (4.4 mm).

Figure 2 shows the result of split-step simulations [40] with tailored input seed spectrum and the resulting output signal spectrum. The parameters were chosen to match the experimental setup, including the seed spectrum. Optimal saturation without shaping the seed spectrum is reached only either for the center (grey) or the edges (blue) of the amplified signal spectrum. The case of ideally saturated central part allows for the use of thinner crystals, but suffers in terms of spectral bandwidth and conversion efficiency. In the case of good saturation at the spectral edges, the central part already starts to be back-converted to the pump pulse, therefore energy and thus efficiency is reduced. A tailored transmission modulation function (orange) decreases the input spectral amplitude of these back-converted signal wavelengths and thus optimizes saturation at all wavelength.

These simulations predict an improvement in energy for this specific case compared to the back-converted case by 14% and to the centrally well saturated case 7%. The Fourier-transform limit (FTL) of the spectra in Fig. 2(c) improves from 8.2 fs for only centrally well saturated

Optics EXPRESS

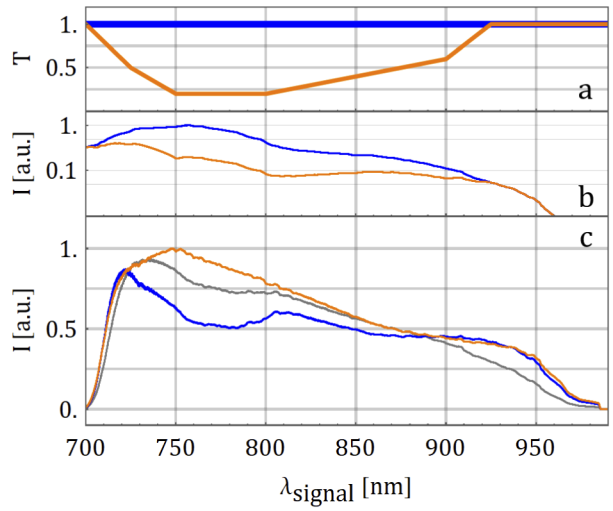

Fig. 2. Simulated effect of seed spectral modulation on OPCPA output in BBO ($I_s(0) = 6\text{MW/cm}^2, I_p(0) = 6\text{GW/cm}^2, t_{\text{FWHM}} = 80$ ps, $\lambda_p = 532$ nm, $\theta = 23.7°$, $\phi = 90°, \alpha = 2.3°$). (a) transmission function of optimal (orange) and unaltered seed (blue), (b) corresponding seed spectra, and (c) amplified spectra at 4.2 mm crystal depth without modulation (grey), and at 4.7 mm without/with modulation (blue/orange).

(grey) to 7.8 fs for back-converted case (blue) and 7.9 fs for optimal case (orange). The peak intensity after compression increases with optimization compared to both non-ideal cases by approximately 12-13%.

The principle of optimal saturation is demonstrated in Fig. 3. It shows the temporally-resolved depletion of the pump pulse on the central transverse axis as a funtion of crystal depth. The maximum pump depletion for different times during the pump pulse is equivalent to the strongest saturation of a corresponding wavelength of the chirped signal pulse. The horizontal axis is signal wavelength, which is a strcitly monotonic funtion of time, because the group delay generated

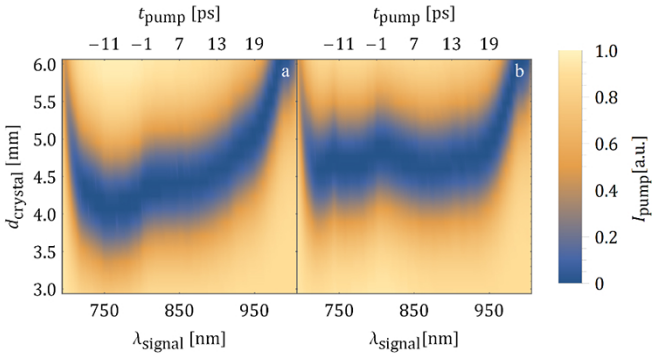

Fig. 3. Simulated temporally-resolved pump depletion for varying BBO crystal lengths ($I_s(0) = 6\text{MW/cm}^2, I_p(0) = 6\text{GW/cm}^2, t_{\text{FWHM}} = 80$ ps, $\lambda_p = 532$ nm, $\theta = 23.7°, \phi = 90°, \alpha = 2.3°$). Depleted temporal pump intensity after amplification vs. signal wavelength or equivalently pump-seed delay and crystal depth with unaltered transmission (a) and optimal transmission modulation function (b). The time within the pump pulse is mapped to a corresponding chirped signal wavelength.

Optics EXPRESS

by the stretcher also depends strictly monotonically on signal wavelength [33]. Figure 3(a) indicates that without controlling the seed spectrum the depth in the crystal for optimal saturation is wavelength dependent, while Fig. 3(b) shows that the optimal seed spectrum minimizes the pump intensity at the same crystal depth for all times, i.e. signal wavelengths.

In principle, the amplification can be even more strongly driven into back-conversion as further reduction of certain seed spectral components compensates it resulting in even higher energy increase and broader spectrum as we will discuss later. However, optical parametric fluorescence, which leads to worse temporal intensity contrast, sets a practical limit to this technique. Typically, the useful regime of spectral seed reduction is up to a factor of 10.

4. Setup

The principle has been experimentally demonstrated with the Light Wave Synthesizer 20 (LWS-20) Optical Parametric Synthesizer (OPS) [24]. The front end including a Ti:Sa oscillator, multi-pass chirped-pulse amplifier, hollow-core fiber and cross-polarized wave generation unit provides a broadband seed. These seed pulses after passing through a grism stretcher [41] and a Dazzler (acousto-optic programmable dispersive filter) [42,43] for phase and amplitude control have about 200 nJ pulse energy and a spectrum supporting sub-5-fs amplified pulses at the end of the system, see also Fig. 4. They are subsequently amplified in two complementary spectral regions by two different sets of noncollinear OPCPA stages and pumped by the second and third harmonic of a Nd:YAG pump laser. At the output of the system, the energy is 75 mJ with a compressed pulse duration of 4.5 fs [24].

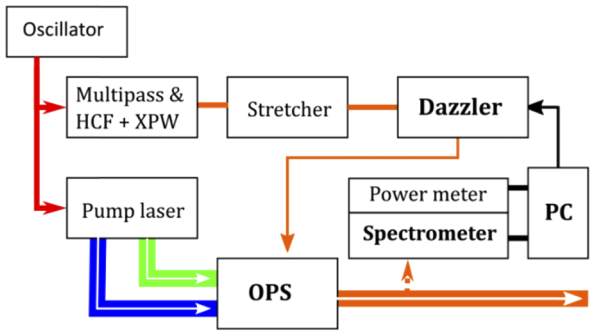

Fig. 4. Experimental setup with an optical parametric synthesizer (OPS) and feedback loop, incorporating the Dazzler, OPS setup and metrology. Multi-pass: kHz Ti:Sa laser, HCF & XPW: hollow-core fiber with cross-polarized wave generation stage.

5. Experiment

As discussed in the theory section, optimization for broadband amplification leads to spectrally dependent small-signal gain in the setup. This together with spectral intensity variation of the seed makes strong back conversion in certain parts of the spectrum unavoidable, while other parts reach optimal depletion. The input spectrum at these back-converted parts has to be decreased.

In Fig. 5 an example for a significant impact of the seed modulation is demonstrated for the 2ω pumped spectral region. Figure 5(c) shows the amplified signal in a spectral window from 700 nm to 980 nm. Independent energy measurements with an energy meter support an increase of energy from 47.5 ± 0.3 mJ to 56.5 ± 0.3 mJ, which corresponds to an improvement by 18.9%. The Fourier limit changes from 8.7 fs to 8.9 fs. It should be noted that the transmission modulation function for the OPS for the spectral part from 700 nm to 990 nm determined by simulations [Fig. 2(a)] and the experiment [Fig. 5(a)] are in very good agreement. This indicates

Optics EXPRESS

good and realistic simulations and understanding of the amplification process. The improvement in this measurement was limited by the maximum suppression of certain spectral components of 5, which still provides a good temporal contrast (8 orders of magnitude at 10 ps [24]). It should be noted, that even 60-80% energy improvement has been measured for very high saturation in a third amplifier stage and an optimal spectral seed transmission. However, the applied maximum suppression of 25 of certain spectral components degraded the contrast to 5.5 orders of magnitude at 10 ps.

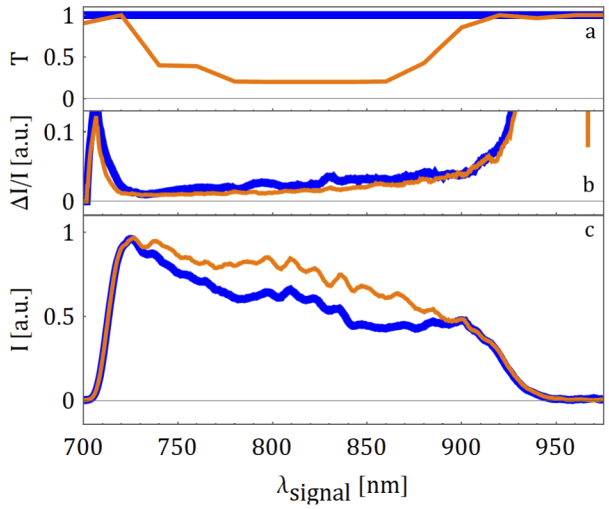

Fig. 5. Experimental data with optimized seed transmission (orange) and with unaltered seed transmission (blue). (a) transmission modulation functions, (b) relative spectral fluctuations, and (c) amplified spectra after OPCPA for the two cases.

6. Spectral and energy stability

In the unsaturated regime fluctuations in the pump pulse energy translate into gain dependent fluctuations of the signal output. An estimate of this relative fluctuation using Eqs. (1) and (2) is given by the formula

$$G\left(1+\frac{\Delta G}{G}\right)=e^{\alpha\sqrt{1+x}}\approx G\left(1+\frac{x\alpha}{2}\right)\qquad\frac{\Delta G}{G}=\frac{x\ln G}{2},\tag{3}$$

where $G = e^{\alpha}$, and $x = \Delta E_{\text{pump}}/E_{\text{pump}}$ correspond to the relative pump laser energy fluctuation. On the contrary, the pump fluctuations in the depletion regime translate 1:1 to the output signal fluctuations, as all input pump is converted into signal and idler. Consequently, an optimization of the transmission modulation function should lead to improved stability for $G > 10$ and depleted spectral components.

The RMS energy stability of the pump laser at 532 nm is about 0.4%. Considering a total small-signal gain in all OPS stages of about 60 dB, according to Eq. (3) the small-signal gain fluctuations are 2.5–3.0%. Experimentally signal energy fluctuations are below 1%, giving evidence for fluctuation suppression via saturation.

In Fig. 5(b) the shot-to-shot RMS spectral intensity fluctuations of 30 consecutively measured spectra are plotted. It demonstrates successful suppression of fluctuations in the spectrum. With unaltered transmission (blue) already back-converted spectral components suffer from stronger fluctuations. Back-conversion takes place from 750 nm to 900 nm as the transmission modulation

Optics EXPRESS

function (orange) in Fig. 5(a) indicates. The spectrum is optimally saturated in this spectral region after optimization and the spectral fluctuations are slightly reduced, which is clearly visible for the above components. Independent measurements with an energy meter show a small improvement from 0.65% to 0.58% energy fluctuation.

7. Application

This approach works also for the whole LWS-20 optical parametric synthesizer, including two different pump wavelengths. The optimal OPCPA seed is determined by systematically scanning the global transmission of the Dazzler and recording the output spectrum of the OPS for each transmission value. The optimal spectral transmission for each spectral component is obtained from this scan. In a next step the Dazzler spectral transmission is then adjusted accordingly, forming a feedback loop (see Fig. 4). We automated this whole procedure, retrieving repeatable and stable results within 1-2 minutes. This can be performed on a daily basis, if the OPS seed changes due to different alignments in the front end. A typical result of such an optimization is shown in Fig. 6 from a different day then the former observation in Fig. 5.

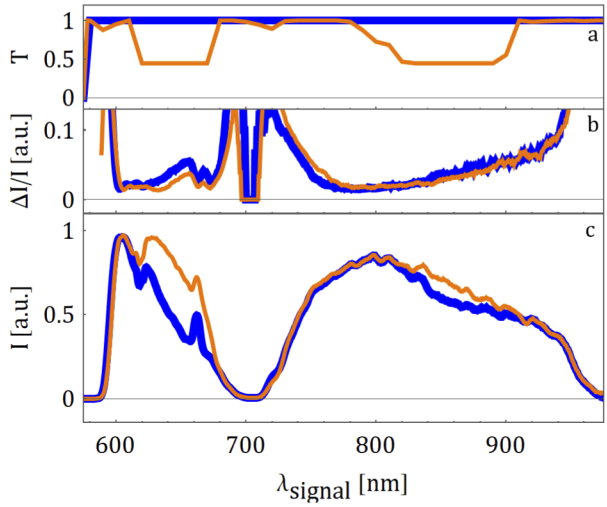

Fig. 6. Experimental data with optimal seed transmission (orange) and with unaltered seed transmission (blue). (a) transmission modulation functions, (b) relative spectral fluctuations, and (c) amplified spectra after OPS for the two cases.

In Fig. 6 11% improvement is shown, in this case significant enhancement is found in two spectral regions, 625 nm to 675 nm and 825 nm to 900 nm. Overall, the energy improves in this case from 71 mJ to 79 mJ and the FTL is for both cases 4.3 fs.

It should be noted that this procedure does not provide improvement for a non-well operated OPCPA system, which is only partially saturated see Fig. 2(c) grey line. Nonetheless, if the amplification is more saturated, see Fig. 2(c) blue line, a broader spectrum with lower energy is obtained. In this case the procedure works and delivers best results, see Fig. 2(c) orange, with similarly broad spectrum and even more energy than the not-well operated case.

8. Conclusion

A simple way to increase the energy, improve the efficiency and reduce the spectral intensity fluctuations of OPCPA systems is demonstrated. Experimental results supported by numerical simulations are presented to optimize the seed spectrum by a spectral shaper that provides the

Optics EXPRESS

conformal seed temporal profile and thus leads up to 20% energy increase and lower spectral fluctuations. Additionally, the amplified bandwidth is potentially broader. This technique can be applied to any OPCPA system with some kind of programmable shaper or possibly even a passive optical element in the seed. The achievable energy enhancement is increasing with amplified bandwidth and gain.

Funding. Kempestiftelserna; Vetenskapsrådet (2016-05409, 2019-02376).

Disclosures. The authors declare no conflicts of interest

References

1. J. A. Armstrong, N. Bloembergen, J. Ducuing, and P. S. Pershan, "Interactions between Light Waves in a Nonlinear Dielectric," Phys. Rev. **127**(6), 1918–1939 (1962).
2. R. A. Baumgartner and R. L. Byer, "Optical Parametric Amplification," IEEE J. Quantum Electron. **15**(6), 432–444 (1979).
3. A. Dubietis, G. Jonusauskas, and A. Piskarskas, "Powerful femtosecond pulse generation by chirped and stretched pulse parametric amplification in BBO crystal," Opt. Commun. **88**(46), 437–440 (1992).
4. S. Witte, R. T. Zinkstok, A. L. Wolf, W. Hogervorst, W. Ubachs, and K. S. E. Eikema, "A source of 2 terawatt, 2.7 cycle laser pulses based on noncollinear optical parametric chirped pulse amplification," Opt. Express **14**(18), 8168–8177 (2006).
5. S. Adachi, N. Ishii, T. Kanai, A. Kosuge, J. Itatani, Y. Kobayashi, D. Yoshitomi, K. Torizuka, and S. Watanabe, "5-fs, multi-mJ, CEP-locked parametric chirped-pulse amplifier pumped by a 450-nm source at 1 kHz," Opt. Express **16**(19), 14341–14352 (2008).
6. D. Herrmann, L. Veisz, R. Tautz, F. Tavella, K. Schmid, V. Pervak, and F. Krausz, "Generation of sub-three-cycle, 16 TW light pulses by using noncollinear optical parametric chirped-pulse amplification," Opt. Lett. **34**(16), 2459–2461 (2009).
7. T. Stanislauskas, R. Budriūnas, R. Antipenkov, A. Zaukevičius, J. Adamonis, A. Michailovas, L. Giniūnas, R. Danielius, A. Piskarskas, and A. Varanavičius, "Table top TW-class OPCPA system driven by tandem femtosecond Yb:KGW and picosecond Nd:YAG lasers," Opt. Express **22**(2), 1865–1870 (2014).
8. S. Prinz, M. Haefner, C. Y. Teisset, R. Bessing, K. Michel, Y. Lee, X. T. Geng, S. Kim, D. E. Kim, T. Metzger, and M. Schultze, "CEP-stable, sub-6 fs, 300-kHz OPCPA system with more than 15 W of average power," Opt. Express **23**(2), 1388–1394 (2015).
9. R. Budriūnas, T. Stanislauskas, J. Adamonis, A. Aleknavičius, G. Veitas, D. Gadonas, S. Balickas, A. Michailovas, and A. Varanavičius, "53 W average power CEP-stabilized OPCPA system delivering 55 TW few cycle pulses at 1 kHz repetition rate," Opt. Express **25**(5), 5797–5806 (2017).
10. S. Sartania, Z. Cheng, M. Lenzner, G. Tempea, C. Spielmann, F. Krausz, and K. Ferencz, "Generation of 0.1-TW 5-fs optical pulses at a 1-kHz repetition rate," Opt. Lett. **22**(20), 1562–1564 (1997).
11. S. Backus, R. Bartels, S. Thompson, R. Dollinger, H. C. Kapteyn, and M. M. Murnane, "High-efficiency, single-stage 7-kHz high-average-power ultrafast laser system," Opt. Lett. **26**(7), 465–467 (2001).
12. B. Bergues, D. E. Rivas, M. Weidman, A. A. Muschet, W. Helml, A. Guggenmos, V. Pervak, U. Kleineberg, G. Marcus, R. Kienberger, D. Charalambidis, P. Tzallas, H. Schröder, F. Krausz, and L. Veisz, "Tabletop nonlinear optics in the 100-eV spectral region," Optica **5**(3), 237–242 (2018).
13. D. E. Cardenas, T. M. Ostermayr, L. D. Lucchio, L. Hofmann, M. F. Kling, P. Gibbon, J. Schreiber, and L. Veisz, "Sub-cycle dynamics in relativistic nanoplasma acceleration," Sci. Rep. **9**, 7321 (2019).
14. D. Kormin, A. Borot, G. Ma, W. Dallari, B. Bergues, M. Aladi, I. B. Földes, and L. Veisz, "Spectral interferometry with waveform-dependent relativistic high-order harmonics from plasma surfaces," Nat. Commun. **9**, 4992 (2018).
15. A. V. Mitrofanov, A. A. Voronin, D. A. Sidorov-Biryukov, A. Pugžlys, E. A. Stepanov, G. Andriukaitis, T. Flöry, S. Ališauskas, A. B. Fedotov, A. Baltuška, and A. M. Zheltikov, "Mid-infrared laser filaments in the atmosphere," Sci. Rep. **5**, 8368 (2015).
16. J. Pupeikis, P.-A. Chevreuil, N. Bigler, L. Gallmann, C. R. Phillips, and U. Keller, "Water window soft x-ray source enabled by a 25 W few-cycle 22 µm OPCPA at 100 kHz," Optica **7**(2), 168–171 (2020).
17. A. Dubietis, R. Butkus, and A. P. Piskarskas, "Trends in chirped pulse optical parametric amplification," IEEE J. Sel. Top. Quantum Electron. **12**(2), 163–172 (2006).
18. S. Witte and K. S. E. Eikema, "Ultrafast optical parametric chirped-pulse amplification," IEEE J. Sel. Top. Quantum Electron. **18**(1), 296–307 (2012).
19. G. Cerullo and S. D. Silvestri, "Ultrafast optical parametric amplifiers," Rev. Sci. Instrum. **74**(1), 1–18 (2003).
20. G. Andriukaitis, T. Balčiūnas, S. Ališauskas, A. Pugžlys, A. Baltuška, T. Popmintchev, M.-C. Chen, M. M. Murnane, and H. C. Kapteyn, "90 GW peak power few-cycle mid-infrared pulses from an optical parametric amplifier," Opt. Lett. **36**(15), 2755–2757 (2011).
21. Y. Deng, A. Schwarz, H. Fattahi, M. Ueffing, X. Gu, M. Ossiander, T. Metzger, V. Pervak, H. Ishizuki, T. Taira, T. Kobayashi, G. Marcus, F. Krausz, R. Kienberger, and N. Karpowicz, "Carrier-envelope-phase-stable, 12 mJ, 15 cycle laser pulses at 21 µm," Opt. Lett. **37**(23), 4973–4975 (2012).

Optics EXPRESS

22. U. Elu, T. Steinle, D. Sánchez, L. Maidment, K. Zawilski, P. Schunemann, U. D. Zeitner, C. Simon-Boisson, and J. Biegert, "Table-top high-energy 7 μm OPCPA and 260 mJ Ho:YLF pump laser," Opt. Lett. **44**(13), 3194–3197 (2019).
23. L. von Grafenstein, M. Bock, D. Ueberschaer, E. Escoto, A. Koç, K. Zawilski, P. Schunemann, U. Griebner, and T. Elsaesser, "Multi-millijoule, few-cycle 5 μm OPCPA at 1 kHz repetition rate," Opt. Lett. **45**(21), 5998–6001 (2020).
24. D. E. Rivas, A. Borot, D. E. Cardenas, G. Marcus, X. Gu, D. Herrmann, J. Xu, J. Tan, D. Kormin, G. Ma, W. Dallari, G. D. Tsakiris, I. B. Földes, S. W. Chou, M. Weidman, B. Bergues, T. Wittmann, H. Schröder, P. Tzallas, D. Charalambidis, O. Razskazovskaya, V. Pervak, F. Krausz, and L. Veisz, "Next Generation Driver for Attosecond and Laser-plasma Physics," Sci. Rep. **7**, 5224 (2017).
25. J. H. Sung, H. W. Lee, J. Y. Yoo, J. W. Yoon, C. W. Lee, J. M. Yang, Y. J. Son, Y. H. Jang, S. K. Lee, and C. H. Nam, "42 PW, 20 fs Ti:sapphire laser at 0.1 Hz," Opt. Lett. **42**(11), 2058–2061 (2017).
26. M. Kretschmar, J. Tuemmler, B. Schütte, A. Hoffmann, B. Senfftleben, M. Mero, M. Sauppe, D. Rupp, M. J. J. Vrakking, I. Will, and T. Nagy, "Thin-disk laser-pumped OPCPA system delivering 44 TW few-cycle pulses," Opt. Express **28**(23), 34574–34585 (2020).
27. J. Ma, J. Wang, B. Zhou, P. Yuan, G. Xie, K. Xiong, Y. Zheng, H. Zhu, and L. Qian, "Broadband, efficient, and robust quasi-parametric chirped-pulse amplification," Opt. Express **25**(21), 25149–25164 (2017).
28. H. Fattahi, "Yb:YAG-PumpedFew-Cycle Optical Parametric Amplifiers," in High Energy and Short Pulse Lasers, Richard Viskup, Ed. (Intech, 2016), pp. 55–72.
29. H. Cao, S. Tóth, M. Kalashnikov, V. Chvykov, and K. Osvay, "Highly efficient, cascaded extraction optical parametric amplifier," Opt. Express **26**(6), 7516–7527 (2018).
30. J. Adamonis, R. Antipenkov, J. Kolenda, A. Michailovas, A. P. Piskarskas, A. Varanavičius, and A. Zaukevičius, "Formation of flat-top picosecond pump pulses for OPCPA systems by cascade second harmonic generation," Lith. J. Phys. **52**(3), 193–202 (2012).
31. T. Balčiūnas, G. Y. Fan, G. Andriukaitis, A. Pugžlys, and A. Baltuška, "High-power top-hat pulses from a Yb master oscillator power amplifier for efficient optical parametric amplifier pumping," Opt. Lett. **37**(13), 2547–2549 (2012).
32. K. Mecseki, D. Bigourd, S. Patankar, N. H. Stuart, and R. A. Smith, "Flat-top picosecond pulses generated by chirped spectral modulation from a Nd:YLF regenerative amplifier for pumping few-cycle optical parametric amplifiers," Appl. Opt. **53**(10), 2229–2235 (2014).
33. J. Rothhardt, S. Hädrich, T. Gottschall, J. Limpert, A. Tünnermann, M. Rothhardt, M. Becker, S. Brückner, and H. Bartelt, "Generation of flattop pump pulses for OPCPA by coherent pulse stacking with fiber Bragg gratings," Opt. Express **17**(18), 16332–16341 (2009).
34. D. Bigourd, P. Morin, J. Dubertrand, C. Dutin, H. Maillotte, Y. Quiquempois, G. Bouwmans, and E. Hugonnot, "Parametric gain shaping from a structured pump pulse," IEEE Photonics Technol. Lett. **31**(3), 214–217 (2019).
35. L. J. Waxer, V. Bagnoud, I. A. Begishev, M. J. Guardalben, J. Puth, and J. D. Zuegel, "High-conversion-efficiency optical parametric chirped-pulse amplification system using spatiotemporally shaped pump pulses," Opt. Lett. **28**(14), 1245–1247 (2003).
36. J. A. Fülöp, Z. Major, B. Horváth, F. Tavella, A. Baltuška, and F. Krausz, "Shaping of picosecond pulses for pumping optical parametric amplification," Appl. Phys. B: Lasers Opt. **87**(1), 79–84 (2007).
37. J. Moses and S.-W. Huang, "Conformal profile theory for performance scaling of ultrabroadband optical parametric chirped pulse amplification," J. Opt. Soc. Am. B **28**(4), 812–831 (2011).
38. I. A. Begishev, A. A. Gulamov, E. A. Erofeev, E. A. Ibragimov, S. R. Kamalov, T. Usmanov, and A. D. Khadzhaev, "Highly efficient parametric amplification of optical beams. I. Optimization of the profiles of interacting waves in parametric amplification," Sov. J. Quantum Electron **20**(9), 1100–1103 (1990).
39. G. Arisholm, "General numerical methods for simulating second-order nonlinear interactions in birefringent media," J. Opt. Soc. Am. B **14**(10), 2543–2549 (1997).
40. T. Lang, A. Harth, J. Matyschok, T. Binhammer, M. Schultze, and U. Morgner, "Impact of temporal, spatial and cascaded effects on the pulse formation in ultra-broadband parametric amplifiers," Opt. Express **21**(1), 949–959 (2013).
41. J. Tan, N. Forget, A. Borot, D. Kaplan, P. Tournois, A. Muschet, and L. Veisz, "Dispersion control for temporal contrast optimization," Opt. Express **26**(19), 25003–25012 (2018).
42. D. Kaplan and P. Tournois, "Theory and performance of the acousto optic programmable dispersive filter used for femtosecond laser pulse shaping," J. Phys. IV **12**(5), 69–75 (2002).
43. P. Tournois, "Acousto-optic programmable dispersive filter for adaptive compensation of group delay time dispersion in laser systems," Opt. Commun. **140**(4-6), 245–249 (1997).